

Electronic Hong-Ou-Mandel interferometer for multi-mode entanglement detection

Vittorio Giovannetti, Diego Frustaglia, and Fabio Taddei
NEST-CNR-INFM and Scuola Normale Superiore, I-56126 Pisa, Italy

Rosario Fazio
International School for Advanced Studies (SISSA), via Beirut 2-4, I-34014 Trieste, Italy
NEST-CNR-INFM and Scuola Normale Superiore, I-56126 Pisa, Italy

(Dated: February 18, 2008)

We show that multi-mode entanglement of electrons in a mesoscopic conductor can be detected by a measurement of the zero-frequency current correlations in an electronic Hong-Ou-Mandel interferometer. By this means, one can further establish a lower bound to the entanglement of formation of two-electron input states. Our results extend the work of Burkard and Loss [Phys. Rev. Lett. **91**, 087903 (2003)] to many channels and provide a way to test the existence of entangled states involving *both* orbital and spin degrees of freedom.

PACS numbers: 03.67.-a, 03.67.Mn, 72.70.+m, 73.23.-b

I. INTRODUCTION

Differently from quantum optics, where entangled photons are routinely detected by coincidence measurements, the issue of revealing the presence of entangled states in multi-terminal mesoscopic conductors (see, e.g., Ref. 1 and references therein) is still an experimental challenge. A number of theoretical proposals have been considered so far. Bell-like tests by means of measurements of current-fluctuations have been analyzed by several authors². Quantum state tomography has been discussed in Ref. 3. Alternatively, Burkard *et al.*⁴ suggested that singlet and triplet electron pairs could give rise to deviations in the zero-frequency shot noise at the output ports of a 50/50 electronic beam splitter (BS) as compared to the value observed for an incoming beam of independent electrons. Following this work, the full counting statistics for entangled electrons in a BS has been studied in Ref. 5. The effect of a Rashba spin-orbit term or a rotating magnetic field in one of the incoming ports was discussed in Refs. 6 and 7, respectively, and in Ref. 8 dephasing through additional reservoirs was included. While these works considered only singlet or triplet incoming states, in Ref. 9 the case of states generated in an Andreev double dot entangler at the input ports of the BS has been discussed.

Our work is motivated by a recent paper by Burkard and Loss¹⁰ where the authors derived a lower bound for the entanglement of formation¹¹ of arbitrary mixed spin states, through shot-noise measurements. In this paper we generalize their results to multi-mode input states by introducing the electronic analog of the Hong-Ou-Mandel (HOM)¹² optical interferometer. We assume that a two-electron (possibly entangled) input state is injected into a BS whose arms support many propagating modes, including both orbital and spin degrees of freedom. In this context, we first show that *zero-frequency* noise measurements allow one to detect entanglement for two-electron input states. Then, in the spirit of Ref. 10, we derive a lower bound for the entanglement of formation in the case

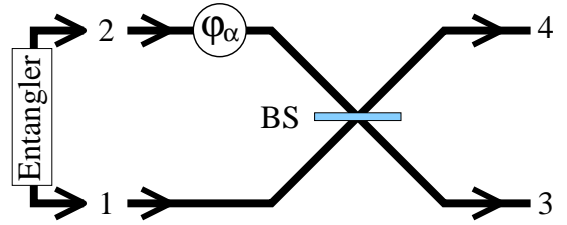


FIG. 1: Schematics of the apparatus. For any energy E , two electrons enter from an entangler at ports 1 and 2. Each port consists of many channels, labeled by a spin (s) and orbital (ℓ) index $\alpha \equiv \{s, \ell\}$. The BS (with transmissivity T that could be controlled by a gate voltage) mixes the incoming state, leading to an outgoing state propagating along ports 3 and 4. Currents are measured at 3 and 4 for different values of a channel-dependent phase shift φ_α introduced in port 2. The presence of spin as well as orbital entanglement in the input state (6) is detected through the Fano factor (7) for current-noise correlations.

of arbitrary number of incoming channels. This is relevant from an experimental point of view since it shows the possibility of characterizing entanglement in complex scenarios which go beyond the paradigmatic two-mode implementation of Burkard and Loss original scheme. Moreover, from a theoretical point of view, our analysis establishes a clear connection between the detection scheme of Ref. 10 and the HOM interferometer scheme proposed in optics.

The main ingredient in the present approach is the study of the oscillations of the zero-frequency shot noise at the outgoing ports of a BS as a function of a controllable phase shift present in one of the incoming ports. As we shall see, this technique allows us to detect spin/orbital as well as more complex entangled input states. In view of its simple implementation we believe this scheme can offer a very convenient way for entanglement detection in mesoscopic multi-terminal conductors.

The paper is organized as follows. In Sec. II we in-

roduce the electronic analog of the HOM interferometer and, in Sec. III, we demonstrate that it detects entanglement for two-electron input states. In Sec. IV we discuss how the zero-frequency noise measurements can be related to the entanglement of formation of the input state. The paper finally ends with conclusions and remarks in Sec. V.

II. THE HOM INTERFEROMETER

In the HOM experiment¹² pairs of multi-mode photons propagating along two distinct optical paths interfere at a 50/50 BS after being phase shifted through controllable delays. The presence of quantum entanglement in the input state of the photons can be recovered by studying the coincidence counts at the output ports of the BS as a function of the relative delay between optical paths. In the electronic analog of the HOM interferometer (e-HOM) metallic conductors play the role of photonic paths and current correlations that of coincidence counts. Apart from the expected differences related to the statistics, the e-HOM interferometer maintains the same entanglement-detection capability of its optical counterpart.

The e-HOM is sketched in Fig. 1. Pairs of electrons of a given energy E above the Fermi sea, prepared in a (possibly entangled) initial state, enter the interferometer from the input ports 1 and 2. Electrons passing through the port 2 undergo an additional, controllable, phase shift (white circle in Fig. 1) before impinging on the BS. Zero frequency current correlations are measured at the output ports 3 and 4. The electron states, at energy E , are labeled by the indices (j, α) where $j = 1, \dots, 4$ labels the ports of the e-HOM interferometer, and where α is the composite index $\{\ell, s\}$ with s referring to electron spin component along the quantization axis, and ℓ referring to the orbital channel. Following the Landauer-Büttiker scattering formulation of quantum transport¹³ we introduce a set of fermionic operators for the incoming $a_{j,\alpha}(E)$ and outgoing $b_{j,\alpha}(E)$ states. They are connected via the scattering matrix by the relation

$$b_{j,\alpha}(E) = \sum_{j'} \mathcal{S}_{j,j'}^{(\alpha)}(E) a_{j',\alpha}(E), \quad (1)$$

where we assume that the spin is conserved in the scattering process and that there is no channel mixing. The phase shifts at the input port 2 are described by the mapping

$$a_{2,\alpha}(E) \rightarrow e^{i\varphi_\alpha} a_{2,\alpha}(E), \quad (2)$$

where φ_α depends on some externally controlled parameters. These transformations can be implemented by introducing local gate voltages and/or magnetic fields at the input port 2, allowing for an independent control of orbital- and spin-related phases, respectively.

In particular, by introducing local electric gatings V_ℓ plus an effective magnetic anisotropy B_{eff} (due to, e.g., spin-orbit coupling⁶), for small perturbations we find $\varphi_\alpha = (eV_\ell/E_\ell)(k_\ell L_0/2) + s(\mu B_{\text{eff}}/E_\ell)(k_\ell L_1/2)$, with k_ℓ the electronic wave-number along the orbital channel ℓ , $E_\ell = (\hbar^2/2m)k_\ell^2$, μ the electronic magnetic moment, $s = \pm 1$ the spin, and L_0 (L_1) the length on which V_ℓ (B_{eff}) acts. For simplicity we will assume a symmetric BS which does not suffer from backscattering. Hence the scattering matrix \mathcal{S} has a block structure of the form

$$\mathcal{S} = \begin{pmatrix} 0 & \mathbb{1} \\ \mathbb{1} & 0 \end{pmatrix} \otimes \hat{s}^{(\alpha)}(E),$$

where $\hat{s}^{(\alpha)}(E)$ describes the transformation of $a_{1,\alpha}(E), a_{2,\alpha}(E)$ into $b_{3,\alpha}(E), b_{4,\alpha}(E)$ and it is expressed by the matrix

$$\hat{s}^{(\alpha)}(E) \equiv \begin{pmatrix} \sqrt{1-T} & \sqrt{T} e^{i\varphi_\alpha} \\ \sqrt{T} & -\sqrt{1-T} e^{i\varphi_\alpha} \end{pmatrix}, \quad (3)$$

where T is the BS transmissivity that could be controlled by, e.g., a gate voltage.¹⁴

The current operator of the j -th port is defined as¹⁵

$$I_j(t) \equiv \frac{e}{h\nu} \sum_{E,\omega,\alpha} e^{-i\omega t} [b_{j,\alpha}^\dagger(E) b_{j,\alpha}(E + \hbar\omega) - a_{j,\alpha}^\dagger(E) a_{j,\alpha}(E + \hbar\omega)], \quad (4)$$

where ν is the density of states of the leads and where a discrete spectrum has been considered to ensure a proper regularization of the current correlations. The zero-frequency current correlations are defined as

$$S_{jj'} = \lim_{T \rightarrow \infty} \frac{h\nu}{T^2} \int_0^T dt_1 \int_0^T dt_2 \langle \delta I_j(t_1) \delta I_{j'}(t_2) \rangle, \quad (5)$$

where the average $\langle \dots \rangle$ is taken over the incoming electronic state, T is the measurement time and $\delta I_j = I_j - \langle I_j \rangle$. We now show that by studying the functional dependence of Eq. (5) upon the phase shifts one can detect the presence of entanglement in the input state of the interferometer.

III. ENTANGLEMENT DETECTION

Consider the *two-electron* case in which, for a given energy E , one electron per port enters the interferometer from 1 and 2. The most general *pure* input state of this form can be expressed as

$$|\Psi\rangle = \prod_E \sum_{\alpha,\beta} \Phi_{\alpha,\beta} a_{1,\alpha}^\dagger(E) a_{2,\beta}^\dagger(E) |0\rangle, \quad (6)$$

where the product is taken for energies in the range $0 < E < eV$, as though ports 1 and 2 were kept at a voltage bias V with respect to ports 3 and 4. Furthermore, $|0\rangle$ is the Fermi sea at zero temperature and $\Phi_{\alpha,\beta}$ is

the two-electron amplitude which we assume to be independent of E and satisfying the normalization condition $\sum_{\alpha,\beta} |\Phi_{\alpha,\beta}|^2 = 1$. One can easily verify that, independently of $\Phi_{\alpha,\beta}$, the average current is constant and equal to $e^2 V/h$. A straightforward calculation of the Fano factor $F_{jj'} = S_{jj'}/(2e\sqrt{\langle I_j \rangle \langle I_{j'} \rangle})$ leads to the expression

$$F_{34} = -T(1-T)(1-w_\Phi), \quad (7)$$

where

$$w_\Phi \equiv \sum_{\alpha,\beta} [\Phi_{\alpha,\beta}]^* \Phi_{\beta,\alpha} e^{i(\varphi_\alpha - \varphi_\beta)} \quad (8)$$

is a (real) quantity which depends on the controllable set of phases $\{\varphi_\alpha\}$. By using the Chauchy-Schwartz inequality and the normalization condition of $\Phi_{\alpha,\beta}$ it follows that for generic input state (6) one has $-1 \leq w_\Phi \leq 1$. However, if $|\Psi\rangle$ in Eq. (6) is a separable state with respect to the input ports 1 and 2, it is possible to show that w_Φ is non negative. In fact, for a separable state (6), the two-electron amplitude factorizes as $\Phi_{\alpha,\beta,\text{sep}} = \chi_\alpha^{(1)} \chi_\beta^{(2)}$ with $\chi_\alpha^{(1)}$ ($\chi_\beta^{(2)}$) being the amplitude associated to the incoming electron of port 1 (2). Replacing this expression in Eq. (8) we get

$$w_{\Phi,\text{sep}} \equiv \left| \sum_{\alpha} [\chi_\alpha^{(1)}]^* \chi_\alpha^{(2)} e^{i\varphi_\alpha} \right|^2 \geq 0. \quad (9)$$

By convexity the same result applies also to any separable mixed state of the form $\rho_{\text{sep}} = \sum_i p_i |\Psi_{\text{sep}}(i)\rangle \langle \Psi_{\text{sep}}(i)|$, with $p_i \geq 0$. Negative values of w_Φ are hence a direct evidence of the presence of entanglement in the input state, i.e.¹⁶

$$\text{If } F_{34} < -T(1-T) \Rightarrow \text{The state is entangled.} \quad (10)$$

Notice that the inverse implication does not hold: indeed there exist entangled states (6) which have w_Φ positive and hence $F_{34} \geq -T(1-T)$ (see Fig. 2 for an example). The quantity w_Φ therefore acts as an *entanglement witness*¹⁷ for the class of two-electron states analyzed here. The condition of Eq. (10) has been derived in Ref. 10 for the spin entangled case. Here we extended its validity to a generic multi-mode entangled input state as defined in Eq. (6). Equation (10) shows that a simple measurement of the Fano factor may be sufficient to ascertain if a given state is entangled. Once the transmissivity T of the BS is known and the phases $\{\varphi_\alpha\}$ are tunable, the test (10) is within current available experimental abilities.

As an example we illustrate in Fig. 2 the detection of the entanglement between two-level electronic states with (pseudo)spin $\alpha = \uparrow, \downarrow$ at, e.g., the output of one of the spin or orbital entanglers so far proposed.¹ By defining $\Phi_{\alpha,\beta} \equiv |\Phi_{\alpha,\beta}| e^{i\eta_{\alpha\beta}}$ we rewrite the quantity in Eq. (8) as

$$w_\Phi = |\Phi_{\uparrow,\uparrow}|^2 + |\Phi_{\downarrow,\downarrow}|^2 + 2|\Phi_{\uparrow,\downarrow}\Phi_{\downarrow,\uparrow}| \cos(\Delta\varphi + \Delta\eta), \quad (11)$$

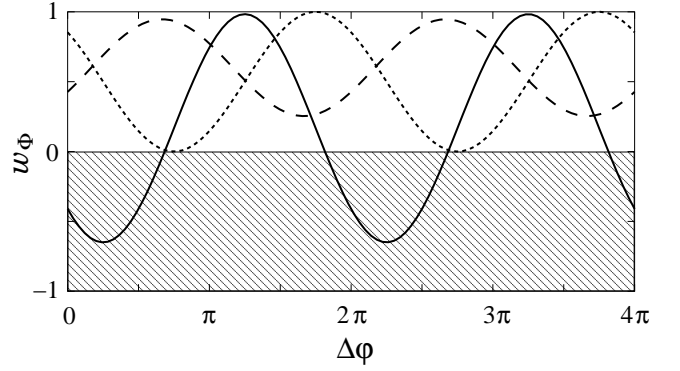


FIG. 2: Entanglement detection scheme applied to the case of two-level electronic states with component $\alpha = \uparrow, \downarrow$. The quantity w_Φ is plotted as a function of $\Delta\varphi = \varphi_\uparrow - \varphi_\downarrow$. A negative w_Φ (shaded area) signals the entanglement in the input state (6). Results are shown for: (solid line) a detectable entangled state with $\Phi_{\uparrow,\downarrow} = 1/\sqrt{2}$, $\Phi_{\downarrow,\uparrow} = e^{i3\pi/4}/\sqrt{3}$, $\Phi_{\uparrow,\uparrow} = \Phi_{\downarrow,\downarrow} = 1/\sqrt{12}$; (dashed line) an undetectable entangled state with $\Phi_{\uparrow,\downarrow} = \Phi_{\downarrow,\uparrow} = \Phi_{\downarrow,\downarrow} = \sqrt{3}/10$, $\Phi_{\uparrow,\uparrow} = e^{-i2\pi/3}/\sqrt{10}$; and (dotted line) a separable state with $\Phi_{\uparrow,\uparrow} = \Phi_{\downarrow,\downarrow} = 1/2$, and $\Phi_{\uparrow,\downarrow} = \Phi_{\downarrow,\uparrow} = e^{i\pi/4}/2$.

with $\Delta\eta \equiv \eta_{\uparrow\downarrow} - \eta_{\downarrow\uparrow}$ and $\Delta\varphi \equiv \varphi_\uparrow - \varphi_\downarrow$. Entanglement can be guaranteed only for those input states leading to a negative w_Φ (shaded area in Fig. 2) for some value of $\Delta\varphi$. We show results for three typical states that can enter the BS analyzer: a detectable entangled state (solid line), an undetectable entangled state (dashed line), and a separable state (dotted line).

IV. LOWER BOUND ON THE ENTANGLEMENT OF FORMATION

Our analysis of the generic input state defined in Eq. (6) proceeds further. By generalizing an argument presented in Ref. 10, in this section we show that the current noise measurement of Eq. (7) is related to the entanglement of formation¹¹ of the input state of the e-HOM interferometer. Fundamental ingredients of our analysis are the d -dimensional *generalized Werner states*^{18,19} whose properties are briefly reviewed in the following for completeness.

A. Generalized Werner stated and generalized twirling transformations

Consider a system composed of two d -dimensional subsystems 1 and 2 and characterized by a separable canonical basis $|\alpha\beta\rangle \equiv |\alpha\rangle_1 \otimes |\beta\rangle_2$ with $\alpha, \beta \in \{1, \dots, d\}$. Following the notation of Ref. 20 we introduce the general-

ized Werner states^{18,19}

$$\sigma_W = \frac{2(1-W)}{d(d+1)} \left(\sum_{\alpha=0}^d |\alpha\alpha\rangle\langle\alpha\alpha| + \sum_{\alpha<\beta} |\Psi_{\alpha\beta}^{(+)}\rangle\langle\Psi_{\alpha\beta}^{(+)}| \right) + \frac{2W}{d(d-1)} \left(\sum_{\alpha<\beta} |\Psi_{\alpha\beta}^{(-)}\rangle\langle\Psi_{\alpha\beta}^{(-)}| \right), \quad (12)$$

with $W \in [0, 1]$ and

$$|\Psi_{\alpha\beta}^{(\pm)}\rangle \equiv \frac{|\alpha\beta\rangle \pm |\beta\alpha\rangle}{\sqrt{2}}. \quad (13)$$

For $d = 2$ Eq. (12) reduces to the standard definition of a qubit Werner state.¹⁹ The entanglement of formation¹¹ E_f of the density matrix σ_W has been computed in Ref. 18. Indeed one can verify that these states are entangled if and only if $W > 1/2$ and that $E_f(\sigma_W) = \mathcal{E}(W)$ with $\mathcal{E}(x)$ being the function

$$\mathcal{E}(x) \equiv \begin{cases} 0 & \text{for } x \in [0, 1/2] \\ H\left(\frac{1+2\sqrt{x(1-x)}}{2}\right) & \text{for } x \in]1/2, 1], \end{cases} \quad (14)$$

(here $H(x) = -x \log_2 x - (1-x) \log_2 (1-x)$ is the binary Shannon entropy). Another important feature of the Werner set (12) is the fact that any input state ρ of the system can be transformed into one of the σ_W by means of Local Operations and Classical Communications (LOCC), i.e.

$$\rho \longrightarrow \sigma_{W(\rho)}, \quad (15)$$

with $W(\rho)$ being the expectation value of the observable $\sum_{\alpha<\beta} |\Psi_{\alpha\beta}^{(-)}\rangle\langle\Psi_{\alpha\beta}^{(-)}|$ on the input state ρ , i.e.

$$W(\rho) = \sum_{\alpha<\beta} \langle\Psi_{\alpha\beta}^{(-)}|\rho|\Psi_{\alpha\beta}^{(-)}\rangle. \quad (16)$$

The map (15) is a *generalized twirling transformation*^{18,20} which can be expressed as follows,

$$T_{\text{wer}}(\rho) \equiv \int dU (U \otimes U) \rho (U^\dagger \otimes U^\dagger) \quad (17)$$

with U being a generic unitary operator on the subsystem and dU being a proper measure in the space of such unitary transformations. It can be shown that Werner states σ_W are fix-points of T_{wer} , i.e. $T_{\text{wer}}(\sigma_W) = \sigma_W$.

By exploiting the properties of T_{wer} , Eq.(15) yields a lower bound to the entanglement of formation of the density matrix ρ . In fact, since the entanglement of a state does not increase under LOCC transformations, we must have

$$E_f(\rho) \geq E_f(\sigma_{W(\rho)}) = \mathcal{E}(W(\rho)), \quad (18)$$

with $\mathcal{E}(x)$ as in Eq. (14). Eq.(18) shows that the quantity $W(\rho)$ of Eq. (16) can be used to bound the entanglement

of ρ . In Sec. IV B we shall prove that the Fano factor (7) with all $\varphi_\alpha = 0$ provides a natural way of measuring the quantity (16) for two-electron input states.

The bound (18) can be strengthened by noticing that the above derivation holds for all choices of the separable canonical basis $|\alpha\beta\rangle$. Indeed for any inequivalent definition of such basis one gets a new set of Werner density matrices and a corresponding new LOCC twirling transformation. Therefore, since $\mathcal{E}(x)$ is non decreasing, Eq. (18) can be replaced by

$$E_f(\rho) \geq \mathcal{E}(\overline{W}(\rho)), \quad (19)$$

where $\overline{W}(\rho)$ is the maximum value of the quantity in Eq. (16) with respect to any possible choice of the separable basis $|\alpha\beta\rangle$. To analyze the performance of the e-HOM set-up we can focus only on those basis which are generated from $|\alpha\beta\rangle$ by applying to subsystem 2 the unitary transformation

$$|\beta\rangle_2 \rightarrow V_2 |\beta\rangle_2 = e^{-i\varphi_\beta} |\beta\rangle_2, \quad (20)$$

with φ_β being one of the controllable phases of the interferometer. The resulting modified Werner states $\tilde{\sigma}_W$ are obtained from Eq. (12) by replacing $|\Psi_{\alpha\beta}^{(\pm)}\rangle$ with the vectors

$$|\tilde{\Psi}_{\alpha\beta}^{(\pm)}\rangle \equiv (e^{-i\varphi_\beta} |\alpha\beta\rangle \pm e^{-i\varphi_\alpha} |\beta\alpha\rangle) / \sqrt{2}, \quad (21)$$

while the corresponding modified twirling transformation is obtained by properly concatenating T_{wer} of Eq. (17) with the unitary phase shifts transformations (20), i.e.

$$\tilde{T}_{\text{wer}}(\rho) \equiv \int dU (U \otimes V_2 U V_2^\dagger) \rho (U^\dagger \otimes V_2 U^\dagger V_2^\dagger).$$

In this context, the $\overline{W}(\rho)$ of Eq. (19) is the maximum of

$$\tilde{W}(\rho) = \sum_{\alpha<\beta} \langle\tilde{\Psi}_{\alpha\beta}^{(-)}|\rho|\tilde{\Psi}_{\alpha\beta}^{(-)}\rangle, \quad (22)$$

for all choices of the phases $\{\varphi_\alpha\}$.

B. Connection with the Fano factor

In the notation of Eq. (6) the states $|\alpha\beta\rangle$ of Eq. (12) can be identified with

$$|\alpha\beta\rangle = \prod_E a_{1,\alpha}^\dagger(E) a_{2,\beta}^\dagger(E) |0\rangle, \quad (23)$$

(this is possible since a_1 and a_2 refer to independent annihilation operators). It is then easy to verify that, assuming ρ to be the input state (6) and exploiting the normalization condition of the two-electron amplitude $\Phi_{\alpha\beta}$, the right hand side of Eq. (22) becomes

$$\tilde{W}(\Psi) = \frac{1 - w_\Phi}{2}, \quad (24)$$

with w_Φ being the quantity in Eq. (8). In particular, setting all the interferometer phases $\{\varphi_\alpha\}$ to zero, we get $W(\rho)$ of Eq. (16). Equation (24) has been explicitly derived for pure input states (6). It can however be generalized to any mixture by linearity. Combining Eqs. (24) and (7) one gets

$$\tilde{W}(\Psi) = -\frac{F_{34}}{2T(1-T)}. \quad (25)$$

This shows that by measuring the Fano factor one can determine $\tilde{W}(\Psi)$ and hence derive a lower bound for the entanglement of formation through Eq. (19).

V. CONCLUSION

In this paper we introduced the fermionic analog of the Hong-Ou-Mandel interferometer. Within this context we discussed the possibility of detecting the presence of multi-mode entanglement for a class of two-electron input states by performing current noise measurements. Following Ref. 10 we also showed that Fano factors measurements provide a natural way of lower bounding the entanglement of formation of such incoming states.

We end with a comparison of the results discussed above with the standard optical HOM interferometer¹² (see also Ref. 21). The optical analog of the two-electron input state (6) is formally obtained by replacing $a_{j,\alpha}(E)$ with bosonic annihilation operators $a_j(k)$ associated with collinear electromagnetic modes of frequency ω_k and propagating along the j -th optical path,²² i.e.

$$|\Psi\rangle = \sum_{k_1, k_2} \Phi_{k_1, k_2} a_1^\dagger(k_1) a_2^\dagger(k_2) |0\rangle, \quad (26)$$

where $|0\rangle$ is now the electromagnetic vacuum (notice the absence of the productory with respect to E). Analogously, the current noise (5) is replaced by the function

$$S_{34} = \lim_{T \rightarrow \infty} \frac{1}{T^2} \int_0^T dt_1 \int_0^T dt_2 \langle \delta I_3(t_1) \delta I_4(t_2) \rangle, \quad (27)$$

which measures coincidence counts fluctuations of the photo-detectors located at the output ports 3 and 4.²³ Replacing Eq. (26) into Eq. (27) gives

$$F_{34} \equiv \frac{S_{34}}{2\sqrt{\langle I_3 \rangle \langle I_4 \rangle}} = -T(1-T)(1+w_\Phi), \quad (28)$$

which should be compared with Eq. (7) of the electronic case (here w_Φ is as in Eq. (8)). The sign difference in front of the function w_Φ is a typical signature of the bunching behavior of bosonic particles.²¹ Nevertheless also in the bosonic case one can use the negativity of w_Φ as a signature of entanglement for the incoming two-photons states (26).

Acknowledgments

This work was supported by the European Community (grants RTN-Spintronics, RTNNANO and EUROSQIP), by MIUR-PRIN, and by the Quantum Information research program of Centro di Ricerca Matematica “Ennio De Giorgi” of Scuola Normale Superiore.

¹ C.W.J. Beenakker, Proceedings XXXX Varenna School on “Quantum computers, algorithms and Chaos” Eprint cond-mat/0508488; G. Burkard, in *Handbook of Theoretical and Computational Nanotechnology*, edited by M. Rieth and W. Schommers (American Scientific Publisher, 2005), Eprint cond-mat/0409626.

² S. Kawabata, J. Phys. Soc. Jpn. **70**, 1210 (2001); N. Chtchelkatchev, G. Blatter, G.B. Lesovik, and T. Martin, Phys. Rev. B **66**, 161320 (2002); P. Samuelsson, E.V. Sukhorukov, and M. Büttiker, Phys. Rev. Lett. **91**, 157002 (2003); C.W.J. Beenakker, C. Emary, M. Kindermann, and J.L. van Velsen, Phys. Rev. Lett. **91**, 147901 (2003); V. Bouchiat, N. Chtchelkatchev, D. Feinberg, G.B. Lesovik, T. Martin, and J. Torres, Nanotechnology **14**, 77 (2003); L. Faoro, F. Taddei, and R. Fazio, Phys. Rev. B **69**, 125326 (2004); A.V. Lebedev, G. Blatter, C.W.J. Beenakker, and G.B. Lesovik, Phys. Rev. B **69**, 235312 (2004). P. Samuelsson, E.V. Sukhorukov, and M. Büttiker, Phys. Rev. Lett. **92**, 026805 (2004).

³ P. Samuelsson, and M. Büttiker, Phys. Rev. B **73**, 041305 (2006).

⁴ G. Burkard, D. Loss, and E.V. Sukhorukov, Phys. Rev. B

61, R16303 (2000).

⁵ F. Taddei and R. Fazio, Phys. Rev. B **65**, 075317 (2002).

⁶ J.C. Egues, G. Burkard, and D. Loss, Phys. Rev. Lett. **89**, 176401 (2002). J.C. Egues, G. Burkard, D. Saraga, J. Schliemann, and D. Loss, Phys. Rev. B **72**, 235326 (2005);

⁷ H. Zhao, X. Zhao, and Y. -Q. Li, Eprint cond-math/0502390;

⁸ P. San José and E. Prada, Eprint cond-mat/0601365.

⁹ P. Samuelsson, E.V. Sukhorukov, and M. Büttiker, Phys. Rev. B **70**, 115330 (2004).

¹⁰ G. Burkard, and D. Loss, Phys. Rev. Lett. **91**, 087903 (2003).

¹¹ C. H. Bennett, D. P. DiVincenzo, J. A. Smolin, and W. K. Wootters, Phys. Rev. A **54**, 3824 (1996); W.K. Wootters, Quantum Inf. Comput. **1**, 3 (2001).

¹² C.K. Hong, Z.Y. Ou, and L. Mandel, Phys. Rev. Lett. **59**, 2044 (1987).

¹³ M. Büttiker, Phys. Rev. B **46**, 12485 (1992).

¹⁴ R.C. Liu, B. Odom, Y. Yamamoto, and S. Tarucha, Nature **391**, 263 (1998).

¹⁵ G. B. Lesovik, Pis'ma Zh. Eksp. Teor. Fiz. **49**, 513 (1989) [JETP Lett. **49**, 592 (1989)].

- ¹⁶ Here there is a subtlety. Due to the non linear dependency upon the currents $\langle I_3 \rangle$ and $\langle I_4 \rangle$ the Fano factor F_{34} is in general not a linear function of the input state. Therefore F_{34} of a convex combination is not necessarily equal to the convex combination of the Fano factors of its components. In our case however $\langle I_3 \rangle$ and $\langle I_4 \rangle$ are constant and do not depend on $|\Psi\rangle$: therefore F_{34} is linear on ρ .
- ¹⁷ M. Horodecki, P. Horodecki, and R. Horodecki, Phys. Lett. A **223**, 1 (1996); M. Lewenstein, B. Kraus, J. I. Cirac, and P. Horodecki, Phys. Rev. A **62**, 52310 (2000).
- ¹⁸ K.G.H. Vollbrecht and R.F. Werner, Phys. Rev. A **64**, 062307 (2001).
- ¹⁹ R.F. Werner, Phys. Rev. A **40**, 4277 (1989).
- ²⁰ S. Lee, D. P. Chi, S. D. Oh, and J. Kim, Phys. Rev. A **68**, 062304 (2003).
- ²¹ V. Giovannetti, Eprint quant-ph/0605223.
- ²² P.G. Kwiat, A.M. Steinberg, and R. Y. Chiao, Phys. Rev. A **45**, 7729 (1992); T.B. Pittman, D. V. Strekalov, A. Migdall, M.H. Rubin, A. V. Sergienko, Y.H. Shih, Phys. Rev. Lett., **77**, 1917 (1996); R. Erdmann, D. Branning, W. Grice, I.A. Walmsley, Phys. Rev. A, **62**, 053810 (2000); V. Giovannetti, L. Maccone, J.H. Shapiro, and F.N.C. Wong, Phys. Rev. Lett., **88**, 183602 (2002); M. Atatüre, G. Di Giuseppe, M.D. Shaw, A.V. Sergienko, B.E.A. Saleh, M.C. Teich, Phys. Rev. A., **65**, 023808 (2002).
- ²³ Here for $j = 3, 4$, $I_j(t)$ is the intensity operator which counts the number of photons impinging on a photo-detector located at the j -th output port. It is given by $I_j(t) = \sum_{k_1} \sum_{k_2} e^{i(\omega_{k_1} - \omega_{k_2})t} b_j^\dagger(k_1) b_j(k_2)$, where $b_j(k)$ is the corresponding bosonic annihilation operator which can be expressed in term of $a_{1,2}(k)$ through a scattering matrix similar to (3).